SAR MOVING TARGET IMAGING USING GROUP SPARSITY

N. Özben Önhon

Turkish-German University
Faculty of Engineering Sciences
Şahinkaya, Beykoz, 34820 Istanbul, Turkey

Müjdat Çetin

Sabancı University
Faculty of Engineering and Natural Sciences
Orta Mahalle, Tuzla, 34956 Istanbul, Turkey

ABSTRACT

SAR imaging of scenes containing moving targets results in defocusing in the reconstructed images if the SAR observation model used in imaging does not take the motion into account. SAR data from a scene with motion can be viewed as data from a stationary scene, but with phase errors due to motion. Based on this perspective, we formulate the moving target SAR imaging problem as one of joint imaging and phase error compensation. Based on the assumption that only a small percentage of the entire scene contains moving targets, phase errors exhibit a group sparse nature, when the entire data for all the points in the scene are handled together. Considering this structure of motion-related phase errors and that many scenes of interest admit sparse representation in SAR imaging, we solve this joint problem by minimizing a cost function which involves two nonquadratic regularization terms one of which is used to enforce the sparsity of the reflectivity field to be imaged and the other is used to exploit the group sparse nature of the phase errors.

Index Terms— SAR, moving target, group sparsity, regularization

1. INTRODUCTION

Synthetic aperture radar (SAR) moving target imaging is a challenging problem, which has attracted great interest in recent years. Moving targets in the scene cause phase errors in the data and subsequently defocusing in the reconstructed image. The defocusing caused by moving targets exhibits space-variant characteristics, i.e., the defocusing arises only in the parts of the image containing the moving targets, whereas the stationary background is not defocused.

For a monostatic spotlight mode SAR which is the case of interest in this paper, a common approach is first to find the smeared imagery of moving targets and then to focus these parts of the image [1–4]. These kinds of approaches are based on post-processing of the conventionally reconstructed image. However, it is known that conventional imaging through, e.g., the polar-format algorithm [5], does not perform well in sparse aperture scenarios or when the data are incomplete.

This work was partially supported by the Scientific and Technological Research Council of Turkey under Grant 105E090, and by a Turkish Academy of Sciences Distinguished Young Scientist Award.

We handle the problem in the context of inverse problems. The original inspiration for the work presented here comes from [6], which presents a method for jointly imaging stationary scenes and correcting phase errors due to, e.g., uncertainties in the sensing platform location. SAR data from a scene with motion can be viewed as data from a stationary scene, but with phase errors due to motion. Accordingly, in our approach, phase errors are regarded as model errors and image formation and phase error compensation are simultaneously performed through iterative minimization of a cost function of both the field and the phase errors. Considering that in SAR imaging, the underlying field usually exhibits a sparse structure, we previosly proposed a sparsity-driven technique for joint SAR imaging and space-variant focusing by using a nonquadratic regularization-based framework [7, 8]. In this technique we have exploited the sparsity of both the reflectivity field and the phase errors, based on the assumption that motion in the scene will be limited to a small number of spatial locations. Actually, phase errors not only have a sparse structure, but they exhibit a group sparse [9] structure as well when the entire data from all the points in the scene are considered and handled together. Here, we modify our previous method using this additional group sparsity information.

Each iteration consists of two steps, the first of which is for image formation and the second is for phase error estimation. Besides effective phase compensation, the proposed technique provides many advantages over conventional imaging as well due to the regularization-based framework. Regularization based imaging techniques can produce images with increased resolution, reduced sidelobes, and reduced speckle by incorporation of prior information about the features of interest and imposing various constraints (e.g., sparsity, smoothness) about the scene.

2. SAR IMAGING MODEL

The SAR discrete imaging model including all returned signals is as follows:

$$\underbrace{\begin{bmatrix} \mathbf{r_1} \\ \vdots \\ \mathbf{r_M} \end{bmatrix}}_{\mathbf{r}} = \underbrace{\begin{bmatrix} \mathbf{C_1} \\ \vdots \\ \mathbf{C_M} \end{bmatrix}}_{\mathbf{C}} \mathbf{f} \tag{1}$$

Here, $\mathbf{r_m}$ is the vector of observed samples, $\mathbf{C_m}$ is a discretized approximation to the continuous observation kernel at the m-th aperture position, $\mathbf{f}$ is a vector representing the unknown sampled reflectivity image and M is the total number of aperture positions. The vector $\mathbf{r}$ is the SAR phase history data of all points in the scene. It is also possible to view $\mathbf{r}$ as the sum of the SAR data corresponding to each point in the scene.

$$\mathbf{r} = \underbrace{\mathbf{C_{cl-1}} f(1)}_{\mathbf{p_1}} + \underbrace{\mathbf{C_{cl-2}} f(2)}_{\mathbf{p_2}} + ... + \underbrace{\mathbf{C_{cl-I}} f(I)}_{\mathbf{p_I}} \tag{2}$$

Here, $\mathbf{C_{cl-i}}$ is the i-th column of the model matrix $\mathbf{C}$ and, $f(i)$ and $\mathbf{p_i}$ represent the complex reflectivity at the i-th point of the scene and the corresponding SAR data, respectively. I is the total number of points in the scene. The cross-range component of the target velocity causes the image of the target to be defocused in the cross-range direction, whereas the range component causes shifting in the cross-range direction and defocusing in both cross-range and range directions [1,2]. The image of a target that experiences significant vibration is defocused in the cross-range direction as well [10]. The defocusing arises due to the phase errors in the SAR data of these targets.

Now, let us view the i-th point in the scene as a point target having a motion which results in defocusing along the cross-range direction. The SAR data of this target can be expressed as [1, 2]:

$$\begin{bmatrix} \mathbf{p_{i_{1_e}}} \\ \mathbf{p_{i_{2_e}}} \\ \vdots \\ \mathbf{p_{i_{M_e}}} \end{bmatrix} = \begin{bmatrix} e^{j\phi_i(1)}\,\mathbf{p_{i_1}} \\ e^{j\phi_i(2)}\,\mathbf{p_{i_2}} \\ \vdots \\ e^{j\phi_i(M)}\,\mathbf{p_{i_M}} \end{bmatrix} \tag{3}$$

Here, $\phi_\mathbf{i}$ represents the phase error caused by the motion of the target and, $\mathbf{p_i}$ and $\mathbf{p_{i_e}}$ are the phase history data for the stationary and moving point target, respectively. In a similar way, this relation can be expressed in terms of the model matrix $\mathbf{C}$ as follows:

$$\begin{bmatrix} \mathbf{C_{cl-i_1}}(\phi) \\ \mathbf{C_{cl-i_2}}(\phi) \\ \vdots \\ \mathbf{C_{cl-i_M}}(\phi) \end{bmatrix} = \begin{bmatrix} e^{j\phi_i(1)}\,\mathbf{C_{cl-i_1}} \\ e^{j\phi_i(2)}\,\mathbf{C_{cl-i_2}} \\ \vdots \\ e^{j\phi_i(M)}\,\mathbf{C_{cl-i_M}} \end{bmatrix} \tag{4}$$

Here, $\mathbf{C_{cl-i}}(\phi)$ is the i-th column of the model matrix $\mathbf{C}(\phi)$ that takes the movement of the targets into account and $\mathbf{C_{cl-i_m}}(\phi)$ is the part of $\mathbf{C_{cl-i}}(\phi)$ for the m-th cross-range position. In the presence of additional observation noise, the observation model for the overall system becomes

$$\mathbf{g} = \mathbf{C}(\phi)\mathbf{f} + \mathbf{v} \tag{5}$$

where, $\mathbf{v}$ is the observation noise. In this way, we have turned the moving target imaging problem into the problem of imaging a stationary scene with phase corrupted data. Here, the aim is to estimate $\mathbf{f}$ and $\boldsymbol{\phi}$ from the noisy observation $\mathbf{g}$.

3. GROUP SPARSITY APPROACH

Particularly considering motions which result in cross-range defocusing, we formulate the problem in a nonquadratic regularization-based framework which allows the incorporation of the prior sparsity information about the field and about the phase errors into the problem. To incorporate the prior information that motion, hence phase errors, are usually present at a small number of spatial location in the scene, and this error is in general observed through data collected at multiple aperture positions, we use a group sparsity constraint in the cost function. The phase errors are incorporated into the problem using the vector $\boldsymbol{\beta}$, which includes phase errors corresponding to all points in the scene, for all aperture positions.

$$\boldsymbol{\beta} = \begin{bmatrix} \boldsymbol{\beta_1} \\ \boldsymbol{\beta_2} \\ \vdots \\ \boldsymbol{\beta_M} \end{bmatrix} \tag{6}$$

Here, $\boldsymbol{\beta_m}$ is the vector of phase errors for the m-th aperture position and has the following form:

$$\boldsymbol{\beta_m} = \left[e^{j\phi_1(m)}, e^{j\phi_2(m)}, ..., e^{j\phi_I(m)} \right]^T \tag{7}$$

Now, let us convert the vector $\boldsymbol{\beta}$ to a matrix so that the columns of this matrix are the $\boldsymbol{\beta_m}$ vectors as follows:

$$\begin{aligned} \mathbf{Q} &= \begin{bmatrix} \boldsymbol{\beta_1} & \boldsymbol{\beta_2} & \dots & \boldsymbol{\beta_M} \end{bmatrix} \\ &= \begin{bmatrix} e^{j\phi_1(1)} & e^{j\phi_1(2)} & \dots & e^{j\phi_1(M)} \\ e^{j\phi_2(1)} & e^{j\phi_2(2)} & \dots & e^{j\phi_2(M)} \\ \vdots & \vdots & \ddots & \vdots \\ e^{j\phi_I(1)} & e^{j\phi_I(2)} & \dots & e^{j\phi_I(M)} \end{bmatrix}_{I \times M} \end{aligned} \tag{8}$$

Here, $\mathbf{Q}$ is the matrix of phase errors and each row of the matrix $\mathbf{Q}$ consists of the phase error values along all aperture positions, for a particular point in the scene. We expect each column of $\mathbf{Q}$ to exhibit sparse nature across the rows, indicating the expectation that there are small number of moving pixels in the scene. However no such sparsity is expected in general across the columns. This structure motivates imposing sparsity in a groupwise fashion, where groups in our setting corresponds to rows of $\mathbf{Q}$.

The method is performed by minimizing the following cost function with respect to the field and phase errors.

$$\begin{aligned} \arg\min_{\mathbf{f},\boldsymbol{\beta}} J(\mathbf{f},\boldsymbol{\beta}) = \arg\min_{\mathbf{f},\boldsymbol{\beta}} & \left\|\mathbf{g} - \mathbf{C}(\phi)\mathbf{f}\right\|_2^2 + \lambda_1 \left\|\mathbf{f}\right\|_1 \\ & + \lambda_2 \sum_{i=1}^{I} \left(\sum_{m=1}^{M} \left| Q(i,m) - 1 \right|^2 \right)^{1/2} \end{aligned} \tag{9}$$

Since the number of moving points is much less than the total number of points in the scene, most of the ϕ values in the vector $\boldsymbol{\beta}$ and subsequently in the matrix $\mathbf{Q}$ are zero. Since the

elements of $\mathbf{Q}$ are in the form of $e^{j\phi}$'s, the elements of the rows corresponding to the stationary scene points become 1, whereas the elements of the rows corresponding to the moving points take various values depending on the amount of the phase error. Therefore, this group sparsity nature on the phase errors is incorporated into the problem by using the regularization term $\sum_{i=1}^{I}\left(\sum_{m=1}^{M}|Q(i,m)-1|^2\right)^{1/2}$.

The proposed algorithm intends to find a local minimum of (9). The algorithm is iterative and at each iteration, in the first step, the cost function $J(\mathbf{f},\boldsymbol{\beta})$ is minimized with respect to the field $\mathbf{f}$:

$$\begin{aligned}\hat{\mathbf{f}}^{(n+1)} &= \arg\min_{\mathbf{f}} J(\mathbf{f},\hat{\boldsymbol{\beta}}^{(n)}) \\ &= \arg\min_{\mathbf{f}} \left\|\mathbf{g}-\mathbf{C}(\phi^{(n)})\mathbf{f}\right\|_2^2 + \lambda_1\|\mathbf{f}\|_1 \end{aligned} \quad (10)$$

To avoid problems due to nondifferentiability of the l_1-norm at the origin, a smooth approximation is used [11]:

$$\|f\|_1 \approx \sum_{i=1}^{I}(|f(i)|^2+\sigma)^{1/2} \quad (11)$$

where σ is a nonnegative small constant. In each iteration, the field estimate is obtained as

$$\hat{\mathbf{f}}^{(n+1)} = \left(\mathbf{C}(\hat{\phi}^{(n)})^H\mathbf{C}(\hat{\phi}^{(n)})+\lambda_1\mathbf{W}(\hat{f}^{(n)})\right)^{-1}\mathbf{C}(\hat{\phi}^{(n)})^H\mathbf{g} \quad (12)$$

where $\mathbf{W}(\hat{f}^{(n)})$ is a diagonal matrix:

$$\mathbf{W}(\hat{f}^{(n)}) = diag\left\{1/\left(\left|\hat{f}^{(n)}(i)\right|^2+\sigma\right)^{1/2}\right\} \quad (13)$$

In the second step of each iteration, we use the field estimate $\hat{\mathbf{f}}$ from the first step and estimate the phase errors by minimizing the following cost function:

$$\begin{aligned}\hat{\boldsymbol{\beta}}^{(n+1)} = \arg\min_{\boldsymbol{\beta}} J(\hat{\mathbf{f}}^{(n+1)},\boldsymbol{\beta}) = \arg\min_{\boldsymbol{\beta}} \left\|\mathbf{g}-\mathbf{H}\mathbf{D}^{(n+1)}\boldsymbol{\beta}\right\|_2^2 \\ +\lambda_2\sum_{i=1}^{I}\left(\sum_{m=1}^{M}|Q(i,m)-1|^2\right)^{1/2}\end{aligned} \quad (14)$$

Here, $\mathbf{H}$ and $\mathbf{D}$ are matrices having the following forms

$$\mathbf{H} = \begin{bmatrix} \mathbf{C_1} & \mathbf{0} & \dots & \dots & \mathbf{0} \\ \mathbf{0} & \mathbf{C_2} & \mathbf{0} & \dots & \mathbf{0} \\ \vdots & \vdots & \vdots & \ddots & \vdots \\ \vdots & \vdots & \vdots & \ddots & \vdots \\ \mathbf{0} & \mathbf{0} & \dots & \mathbf{0} & \mathbf{C_M} \end{bmatrix} \quad (15)$$

where $\mathbf{C_m}$ denotes the submatrix for the part of the model matrix corresponding to the m-th aperture position.

$$\mathbf{D}^{(n+1)} = \begin{bmatrix} \mathbf{T}^{(n+1)} & \mathbf{0} & \dots & \dots & \mathbf{0} \\ \mathbf{0} & \mathbf{T}^{(n+1)} & \mathbf{0} & \dots & \mathbf{0} \\ \vdots & \vdots & \vdots & \ddots & \vdots \\ \vdots & \vdots & \vdots & \ddots & \vdots \\ \mathbf{0} & \mathbf{0} & \dots & \mathbf{0} & \mathbf{T}^{(n+1)} \end{bmatrix} \quad (16)$$

Here, $\mathbf{T}$ is a diagonal matrix, with the entries $\hat{f}(i)$ on its main diagonal, as follows:

$$\mathbf{T}^{(n+1)} = diag\left\{\hat{f}^{(n+1)}(i)\right\} \quad (17)$$

The convex optimization problem in (14) can be efficiently solved via second order cone programming [12]. For the sake of simplicity of the optimization process, in (9) we have not used an additional constraint to force the magnitudes of the vector $\boldsymbol{\beta}$ to be 1. Consequently, since in this step we want to use only the phase information and to suppress the effect of the magnitudes, the estimate $\hat{\boldsymbol{\beta}}$ is first normalized and then for every aperture position the following matrix is created,

$$\mathbf{B_m}^{(n+1)} = diag\left\{\hat{\beta}_m^{(n+1)}(i)\right\} \quad (18)$$

which is used to update the corresponding part of the model matrix.

$$\mathbf{C_m}(\phi^{n+1}) = \mathbf{C_m}\mathbf{B_m}^{(n+1)} \quad (19)$$

After these phase estimation and model matrix update procedures have been completed, the algorithm passes to the next iteration.

4. PRELIMINARY EXPERIMENTAL RESULTS ON SYNTHETIC SCENES

We present preliminary experimental results on three different synthetic scenes. In these experiments the regularization parameters λ_1 and λ_2 are chosen empirically. To demonstrate the performance of the presented approach, for all experiments, the images reconstructed by conventional imaging and sparsity-driven imaging [11] are presented as well.

The results for the Experiment 1, Experiment 2, and Experiment 3 are presented in Figure 1, Figure 2, and Figure 3, respectively. The scene used in the Experiment 1 involves four point targets. The leftmost and the rightmost targets are stationary, whereas the two targets lying in the middle are simulated to have different constant velocities in the cross-range direction. To simulate such motion, the phase history data of the right target are corrupted with a quadratic phase error of a center to edge amplitude of 2.5π radians and the phase history data of the left target are corrupted with a quadratic phase error of a center to edge amplitude of π radians. Similarly, in the second experiment the phase history data of the two large square-shaped targets lying in the middle of the scene are corrupted with a quadratic phase error of a center to edge amplitude of π and 2π radians (from left to right). In the third experiment, a multiple-point target with a different shape is simulated to be moving. The phase error used to corrupt the data is a quadratic phase error of a center to edge amplitude of π radians.

For all of these three scenarios, in the results of conventional imaging and sparsity-driven imaging without any phase

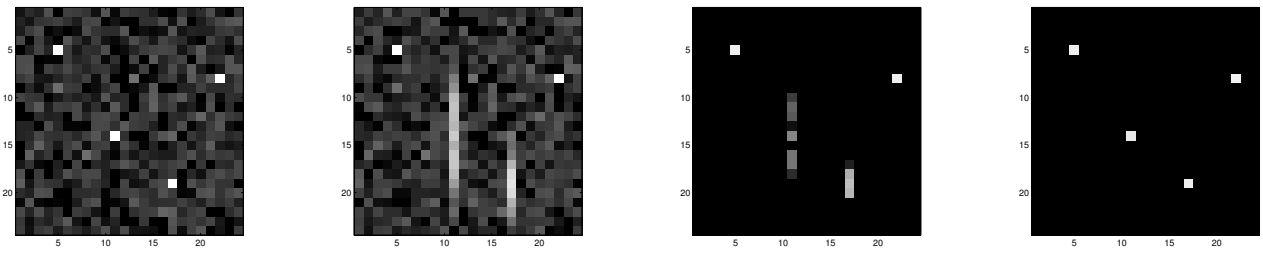

(a) (b) (c) (d)

Fig. 1. a) Original scene. b) Image reconstructed by conventional imaging. c) Image reconstructed by sparsity-driven imaging. d) Image reconstructed by the proposed method.

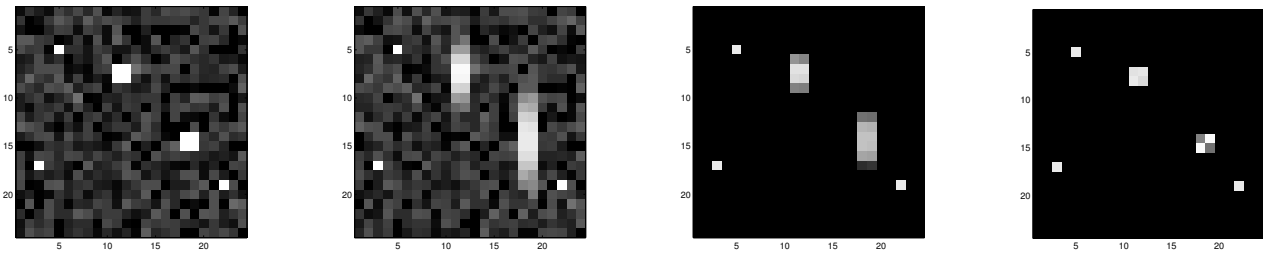

(a) (b) (c) (d)

Fig. 2. a) Original scene. b) Image reconstructed by conventional imaging. c) Image reconstructed by sparsity-driven imaging. d) Image reconstructed by the proposed method.

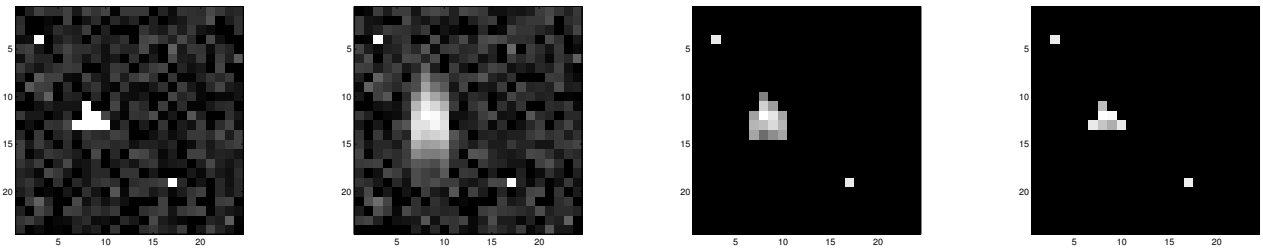

(a) (b) (c) (d)

Fig. 3. a) Original scene. b) Image reconstructed by conventional imaging. c) Image reconstructed by sparsity-driven imaging. d) Image reconstructed by the proposed method.

error correction, the defocusing and artifacts in the reconstructed images caused by the moving targets are clearly seen. On the other hand, our approach produces images with focused targets together with an estimate of the phase errors which is related to the underlying motion of the targets.

5. CONCLUSION

In this work, the SAR moving target imaging problem is posed as an optimization problem. Motion in the scene is modeled through the phase errors it generates on the radar returns that would be collected from a corresponding stationary scene. The presented method is based on minimization of a cost function in which the sparsity of the field and the group sparse nature of the phase errors are imposed using nonquadratic regularization terms. The preliminary results demonstrate that the method can remove the defocusing effect of the phase errors errors caused by motion in the scene, and it also benefits from the advantages offered by sparsity-driven imaging.

6. REFERENCES

[1] C. V. Jakowatz, Jr., D. E. Wahl, and P. H. Eichel, "Refocus of constant velocity moving targets in synthetic aperture radar imagery," *Algorithms for Synthetic Aperture Radar Imagery V, SPIE*, 1998.

[2] J. R. Fienup, "Detecting moving targets in SAR imagery by focusing," *IEEE Transactions on Aerospace and Electronic Systems*, vol. 37, no. 3, pp. 794–809, 2001.

[3] J. K. Jao, "Theory of synthetic aperture radar imaging of a moving target," *IEEE Trans. Geosci. Remote Sens.*, vol. 39, pp. 1984–1992, 2001.

[4] M. J. Minardi, L. A. Gorham, and E. G. Zelnio, "Ground moving target detection and tracking based on generalized SAR processing and change detection," *Proc. SPIE, Algorithms for Synth. Aperture Radar Imagery XII*, vol. 5808, pp. 156–165, 2005.

[5] W. G. Carrara, R. M. Majewski, and R. S. Goodman, *Spotlight Synthetic Aperture Radar: Signal Processing Algorithms*, Artech House, 1995.

[6] N. Ö. Önhon and M. Çetin, "A sparsity-driven approach for joint SAR imaging and phase error correction," *IEEE Transactions on Image Processing*, vol. 21, pp. 2075–2088, 2012.

[7] N. Ö. Önhon and M. Çetin, "Sparsity-driven image formation and space-variant focusing for SAR," *IEEE Int. Conf. on Image Processing (ICIP)*, pp. 173–176, 2011.

[8] N. Ö. Önhon and M. Çetin, "SAR moving target imaging in a sparsity-driven framework," *SPIE Optics+Photonics, Wavelets and Sparsity XIV*, vol. 8138, 2011.

[9] M. Yuan and Y. Lin, "Model selection and estimation in regression with grouped variables," *Journal of Royal Statistical Society:Series B*, vol. 68, pp. 49–67, 2006.

[10] A. R. Fasih, B. D. Rigling, and R. L. Moses, "Analysis of target rotation and translation in SAR imagery," *Algorithms for Synthetic Aperture Radar Imagery XVI, SPIE*, 2009.

[11] M. Çetin and W. C. Karl, "Feature-enhanced synthetic aperture radar image formation based on nonquadratic regularization," *IEEE Trans. Image Processing*, pp. 623–631, 2001.

[12] S. Boyd and L. Vandenberghe, *Convex Optimization*, Cambridge University Press, 2004.